AD-A193 128 CALCULATION OF FAR INFRARED ABSORPTION IN B 1/1
POLY(DA)POLY)(DT)(U) PURDUE UNIV LAFAYETTE IND DEPT OF
PHYSICS L YOUNG ET AL. 10 MAR 88 N00014-86-K-0252
UNCLASSIFIED F/G 6/2 NL

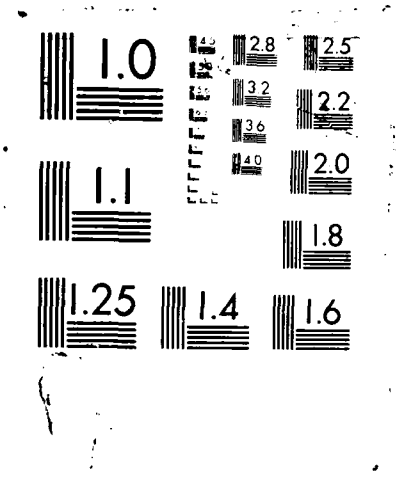
1.0
1.1
1.25
1.4
1.6
1.8
2.0
2.2
2.5
2.8
3.2
3.6
4.0

REPORT DOCUMENTATION PAGE

(2)

NA

Distribution Unlimited

NA

Purdue Research Foundation

Purdue Research Foundation

NA

Technology Applications Programs

W. Lafayette, IN 47907

OSD/SD10/TA
Washington, D.C. 20301-7100

Strategic Defense Initiative Organization

NO0014-86-K-0252

Washington, D.C. 20301-7100

PROGRAM ELEMENT NO	PROJECT NO	TASK NO	WORK UNIT ACCESSION NO
63222C			

Calculation of Far Infrared Absorption in B poly(dA)·poly(dT)

L. Young and E.W. Prohofsky

TYPE OF REPORT	TIME COVERED	DATE OF REPORT (Year, Month, Day)	PAGE COUNT
Technical	FROM 4/81 TO 3/88	1988 - 3-10	

FIELD	GROUP	SUB-GROUP

We calculate the far infrared absorption of B conformation poly(dA)·poly(dT), using eigenvectors from a lattice dynamical model refined with the latest inelastic neutron scattering data. Our various calculations include the isolated helix, the addition of counterions, and the addition of a "spine of hydration" in the minor groove. We find agreement with experimental infrared data except for one mode. We then attempt to model a coupling between two helices and show some evidence that this mode is interhelical.

DISTRIBUTION STATEMENT A
Approved for public release:
Distribution Unlimited

U

Charles L. Houston III

(202)693-1556

OSD/SD10/TA

Calculation of Far Infrared Absorption in B poly(dA) · poly(dT)

L. Young and E. W. Prohofsky

Department of Physics

Purdue University

West Lafayette, Indiana 47907

We calculate the far infrared absorption of B conformation poly(dA) · poly(dT), using eigenvectors from a lattice dynamical model refined with the latest inelastic neutron scattering data. Our various calculations include the isolated helix, the addition of counterions, and the addition of a "spine of hydration" in the minor groove. We find agreement with experimental infrared data except for one mode. We then attempt to model a coupling between two helices and show some evidence that this mode is interhelical.

PACS Numbers: 87.10+e, 63.20-e, 78.30-j

Introduction

Since our initial prediction of vibrational modes in DNA in the 1-100 cm^{-1} frequency range,[1,2] several experimental groups have used Brillouin,[3] low frequency Raman,[4] and infrared absorption[5] measurements to study this region of the spectrum. Resonant rather than dissipative modes have been observed and in one case the lifetime of such a mode has been determined.[3] Infrared absorption has been carried out at both room temperature and at low temperature. The relatively sharp lines available from this measurement have indicated a temperature dependence in agreement with our calculations.[6] The good experimental data has, however, raised new challenges to the theory. Can one achieve good fits and assignments to observed lines in this region? This question implies fitting both the frequency and the relative absorption.

In addition to this new Raman and infrared data, inelastic neutron scattering data is also now available.[7] This neutron data is of particular interest to us as it has allowed refinement of our model of the long range non-bonded interactions in DNA.[8] These non-bonded interactions are the predominant interaction at lowest frequencies; that is, $\nu < 10 cm^{-1}$. The non-bonded interactions are unimportant at higher frequencies ($\nu > 200 cm^{-1}$) where the bonded interactions predominate, yet, they are still important for determining frequencies in the range of interest ($10 < \nu < 200 cm^{-1}$) in this paper. Our earlier model of these non-bonded interactions was fitted to Brillouin scattering observations of the acoustic velocity in DNA at 5-20 GHz in frequency. This is not an entirely satisfactory frequency range for fitting as it is low enough for the effective dielectric constant to be dominated by that of the water near the DNA helix.

The low frequency dielectric constant of water is very large but the higher frequency value is considerably less. Lee, et.al.[10] have used acoustic attenuation data to estimate the rotational relaxation time of water molecules near the DNA helix. They indicate that the nearest layer of water can rotate only up to frequencies $\approx$ 4 GHz, and that bulk water can rotate up to frequencies $\approx$ 80 GHz, the latter in agreement with other estimates of the rotational relaxation time for bulk water.

The 5-20 GHz acoustic data is still in the frequency range where the water dipoles can rotate and effectively sheild electric fields. The inelastic neutron data is at frequencies of hundreds of GHz and, therefore, above the region of large water dielectric response. We were able to use the neutron data to fit a non-bonded interaction model that should be appropriate for even higher frequencies, where the principal element in that model is the electrostatic interaction shielded by a model of dielectric response.[9] Once above the water rotational relaxtion frequency the dielectric constant of water should be a relatively slowly varying parameter. This paper will then use the non-bonded model, based on fitted inelastic neutron scattering data, along with a bonded force constant model, developed by refining higher freqency Raman and infrared data[11] to calculate the frequencies and the absorption of lines in the far infrared in poly(dA) $\cdot$ poly(dT) to compare with the observed far infrared absorption.

As demonstrated by Powell, et.al.[5] relatively sharp infrared lines can be found in good samples of DNA. In these best samples, the DNA is more ordered than in the poorer samples which give rise to much broader absorption peaks. In these more ordered DNA samples, one would expect strong interhelical interactions. Such strong interhelical interactions bring into question the

calculational approximation of a single isolated helix. Previous studies have centered on the intrahelical modes, associated with motions mostly in a single helix. Now, in addition, one has strong likelihood of interhelical modes -- modes in which the interactions between helices are dominant.

For properly analyzing a system having both intra- and inter-helical modes, one must use an entire crystalline unit cell. According to Lindsay[12] such a cell would have at a minimum, two to three-ten base pair sections of helix, plus all the counterions and water of hydration. The secular matrix would be roughly 30x30 larger than our homopolymer matrices. Methods to approximate such calculations are being developed.

In this paper we present a simple set of calculations which are aimed at separating out the intra- and inter-helical modes. We consider how well a simple homopolymer lattice dynamics calculation can predict the frequency and relative absorption of the intrahelical modes. We do this by comparing the isolated helix vibrational modes to those from several calculations in which the helix interacts with its surroundings in increasing detail. These calculations are for interactions with counterions, interactions with water molecules, and then the combination of the two. We find the method works fairly well for those modes we believe to be intrahelical. Furthermore, we develop a crude calculation to predict the frequencies of the helix interacting with another helix in its surroundings -- a calculation of interhelical modes. We find that the principal feature in the measured infrared spectrum that does not correspond to our intrahelical calculations corresponds roughly to a frequency predicted by our crude interhelical calculation.

Calculations of Vibrational Modes

We begin with the application of theories of solid state physics to DNA and model the DNA homopolymer as a one-dimensional infinite lattice (or periodic arrangement of atoms) whose periodic units (or unit cells) are nucleotide pairs or base pairs. The entire double helical homopolymer is generated by taking one base pair and repeating it along the helix axis in the manner of translations and rotations about this axis as if the unit cell were on a screw. In fact, such a lattice is said to have a screw symmetry with a translation operation of p, the pitch of the helix, and a rotation operation of ψ, the pitch angle. Each application of this screw operation yields the next unit cell. Then, according to Bloch's theorem, for an infinite lattice, the motion of the atoms in one repeat unit is the same as that in another except that the two may be of different phase. Therefore, the problem of studying the entire lattice is reduced to the study of one unit cell with all possible phase relationships between succeeding unit cells.

Given the atomic coordinates, masses, charges, and force constants, we find the kinetic and potential energy of the lattice, the equations of motion, and thus, the secular equation as in Eyster and Prohofsky.[13,14] The secular equation is derived in terms of the mass-weighted cartesian displacement coordinates (MWC) q_i:

$$q_i = \sqrt{m_i}\, x_i \,, \tag{1}$$

m_i being the mass of, and x_i the displacement of the i^{th} atom. Then the secular equation is given as

$$| \mathbf{B}^{\dagger}(\theta)\mathbf{F}\mathbf{B}(\theta) \quad \omega^2 \mathbf{I} | \quad 0 \,. \tag{2}$$

$\mathbf{B}^t(\theta)\mathbf{FB}(\theta)$ should actually be written as $[\mathbf{B}^t(\theta)\mathbf{FB}(\theta)]_v + [\mathbf{B}^t(\theta)\mathbf{FB}(\theta)]_{nb}$, where the first term is for valence or bonded force constants, and the second term is for non-bonded interactons.

In $[\mathbf{B}^t(\theta)\mathbf{FB}(\theta)]_v$, $\mathbf{F}$ is the diagonal matrix of force constants of the internal coordinates, S_i. $\mathbf{B}(\theta)$ serves to transform $\mathbf{F}$ to MWC coordinates and also account for the phase difference θ betweeen unit cells n, $\mathbf{B}(\theta) = \sum_n \mathbf{B}^n \mathbf{R}^n e^{in\theta}$, where $\mathbf{R}$ is a rotation matrix. The elements of $\mathbf{B}$ are calculated as in Chapter 4 of Wilson, et.al.[15] The valence force constants are refined by Lu,[11] based on spectral data above 400 cm^{-1}. Thus, the rows of $\mathbf{B}$ correspond to the numbering of internal coordinates and the columns to the numbering of the x,y,z components of the MWC coordinates.

For $[\mathbf{B}^t(\theta)\mathbf{FB}(\theta)]_{nb}$, the same concepts hold for $\mathbf{F}$ and $\mathbf{B}$, although in practice we store the matrix elements somewhat differently. We treat the non-bonded interactions between the two atoms of different unit cells as a stretch internal coordinate. Since all of these interactions are stretches, we do not number the internal coordinates but instead label them according to the atoms involved.

As an example, we compare $\mathbf{B}$ for the bonded term with $\mathbf{B}$ for the non-bonded term. For the bonded term, $B_{3,5}$ corresponds to the third internal coordinate, S_3 and the y component of the MWC coordinate of the second atom (atom 1 components are 1, 2, 3, atom 2 components are 4, 5, 6, ...). If S_3 is a stretch between atoms 2 and 6, $B_{3,4}$, $B_{3,5}$, $B_{3,6}$, $B_{3,16}$, $B_{3,17}$, $B_{3,18}$ will be the only non-zero elements on row three. But in the non-bonded term $\mathbf{B}$ is a three-dimensional matrix, $B_{2,6,2}$ corresponding to the y (or second) component of atom 2 (since the third dimension counts x,y,z for the atom listed in the

first dimension) involved in the stretch with atom 6. Since the non-bonded problem involves around $(40)^2$ stretches and no other type of internal coordinate, the three-dimensional **B** is more compact for computing purposes.

Upon adding these parts together, we can solve the secular equation for the eigenfrequencies and eigenvectors; that is, the resonant frequencies and the relative amplitudes of the atoms of the lattice. Thus we have an adequate expression of its dynamics.

Modification of Non-Bonded Potential Energy

The potential energy comprises bonded and non-bonded terms which leads to $\mathbf{B}^t(\theta)\mathbf{F}\mathbf{B}(\theta) = [\mathbf{B}^t(\theta)\mathbf{F}\mathbf{B}(\theta)]_v + [\mathbf{B}^t(\theta)\mathbf{F}\mathbf{B}(\theta)]_{nb}$. We follow the method of Eyster and Prohofsky[14] in calculating the non-bonded force constants, modifying the functional form:

$$F_{i,j} = F_1 + F_2 \tag{3}$$

$$F_1 = 2\eta \frac{e_i e_j}{\sqrt{\epsilon_i \epsilon_j r_{i,j}^3}}, \tag{4}$$

$$F_2 = 42 \frac{A}{(r_{i,j})^n}, \tag{5}$$

where i and j count atoms in different unit cells. F_1 is for long range or coulombic interactions, the i^{th} atom having a charge e_i, associated with a dielectric screening ϵ_i and separated from atom j by a distance $r_{i,j}$. The charges e_i are taken from calculations by Miller,[16] the hydrogen atoms' charge

(as well as mass) being included in the atoms to which they are attached. The charges are reduced by a factor of 2.31 based on a fit to inelastic neutron scattering data[9] as well as comparison to a few charges determined experimentally by fitting to x-ray scattering data.[17] η =0.43, which includes a conversion factor and the scaling of 2.31 for each charge. The conversion factor is needed because the units of the force constants are $\frac{mdyne}{\text{Å}}$, but the charges are given in units of electronic charge and the coordinates in angstroms. Two distinct dielectric screenings ϵ_i, ϵ_j are used, as some atoms (mostly in the backbone) see each other through water, whereas others (particularly in the bases) see each other through DNA. This difference explains the stronger base-base interactions. We let the dielectric vary linearly according to the distance between the atoms up to an effective separation r_{eff}.[18,19] For distances greater than r_{eff} the dielectric is treated as a constant. If the atom separation is less than the contact distance r_{con} (the minimum separation allowed between the centers of two atoms), the dielectric constant is taken to be unity. We use an effective distance of 10 Å and a contact distance of 2 Å.

The formula for the dielectric function is

$$\epsilon_{ij} = \epsilon_c + \frac{(\epsilon_o - \epsilon_c)}{(r_{eff} - r_{con})}(r_{ij} - r_{con}) . \qquad (6)$$

ϵ_c is the dielectric constant at the contact distance, r_{con}, ϵ_c is the dielectric constant at the effective separation, r_{eff}, and r_{ij} is the separation of atoms i and j. For the interaction between the base atoms, ϵ_o = 6.0. We use ϵ_o = 9.0 for the backbone atoms' interaction. As discussed in the introduction, the choice of a value of 9 for the long range dielectric value of water near DNA is

appropriate to calculations in the THz (30-300cm^{-1}) region. F_2 describes the Van der Waals interaction when n=8. A is the phenomonological parameter adjusted to a value of 0.12 to fit the infrared absorption data. The long range interaction is for the unit cell and nineteen neighbors on either side. The Van der Waals interaction is much shorter in range, involving only one neighbor on each side of the unit cell. The new set of eigenvectors obtained from this refinement are used to calculate the absorption.

Bare DNA Absorption Calculation

We apply the expressions developed by Kohli, et.al.[20] to calculate the absorption of radiation by poly(dA) · poly(dT) which is in the B conformation. For the relative intensity of the peaks, we calculate the Einstein absorption coefficients:

$$B_L = \frac{8\pi^3}{h^2} \mid <\mu_{l\theta}^{L}> \mid^2 \tag{7}$$

$$B_T = \frac{8\pi^3}{h^2} \mid <\mu_{l\theta}^{T}> \mid^2 \tag{8}$$

where L and T refer to the longitudinal (along the helix axis) and transverse (perpendicular to the helix axis) electromagnetic fields and $<\mu_{l\theta}>$ is the transition matrix element of the electric dipole moment operator for the l,θ vibrational mode, l labeling the band and θ, the phase shift from cell to cell.

Assuming the absorption of radiation precipitates a transition between the two lowest vibrational states, these matrix elements are proportional to

$$<\mu_l^L{}_\theta> = \frac{1}{\sqrt{2}} \sum_i \frac{e_i}{\sqrt{m_i}} \left(\frac{\hbar N}{2\omega_{l\theta}} \right)^{\frac{1}{2}} \delta_\theta \, S_{il}^0 \tag{9}$$

$$<\mu_l^T{}_\theta> = \frac{1}{\sqrt{2}} \sum_i \frac{e_i}{\sqrt{m_i}} \left(\frac{\hbar N}{2\omega_{l\theta}} \right)^{\frac{1}{2}} (S_{il}^+ \delta_{\theta-\psi} + S_{il}^- \delta_{\theta+\psi}), \tag{10}$$

the sum being over the atoms of the repeat unit with charge e_i and mass m_i, with N, the number of repeat units or base pairs. Also,

$$\delta_\alpha \equiv \frac{\sin\left(N\frac{\alpha}{2}\right)}{N \sin\left(\frac{\alpha}{2}\right)}, \tag{11}$$

and

$$S_{il}^{\pm} = \frac{q_{ix}^l \pm i q_{iy}^l}{2} e^{\pm i\phi}, \quad S_{il}^0 = q_{iz}^l, \tag{12}$$

where q_{ix}^l, q_{iy}^l, q_{iz}^l are the components of the l^{th} vibrational mode eigenvector and ϕ is the angle the transverse component of the electromagnetic field makes with the $\hat{x}$ direction.

For our case of an infinite chain, the absorption occurs only for $\theta = 0.0$ in equation 9 and $\theta = \pm\psi$ in equation 10, according to Kohli, et.al.[20] Then for each base pair (N=1),

$$<\mu_l^L{}_{\theta=0}> = \frac{1}{\sqrt{2}} \sum_i \frac{e_i}{\sqrt{m_i}} \left(\frac{\hbar}{2\omega_{l\,\theta=0}} \right)^{\frac{1}{2}} q_{iz}^l \tag{13}$$

$$<\mu_l^T{}_{\theta=\pm\psi}> = \frac{1}{\sqrt{2}} \sum_i \frac{e_i}{\sqrt{m_i}} \left(\frac{\hbar}{2\omega_{l\,\theta=\pm\psi}} \right)^{\frac{1}{2}} \frac{q_{ix}^l + i q_{iy}^l}{2} e^{\pm i\phi}, \tag{14}$$

and

$$B_L = \frac{8\pi^3}{\hbar^2} \frac{\hbar}{4\omega_{l,\theta=0}} \left| \sum_i \frac{e_i}{\sqrt{m_i}} q_{ix}^l \right|^2 \tag{15}$$

$$B_T = \frac{8\pi^3}{\hbar^2} \frac{\hbar}{4\omega_{l,\theta=\psi}} \left| \sum_i \frac{e_i}{\sqrt{m_i}} \frac{(q_{ix}^l + iq_{iy}^l)}{2} \right|^2. \tag{16}$$

Noting that $\omega_{l,\theta=+\psi} = \omega_{l,\theta=-\psi}$ (due to time reversal symmetry), and $\left| \sum_i \frac{e_i}{\sqrt{m_i}} (q_{ix}^l + iq_{iy}^l) \right|^2 = \left| \sum_i \frac{e_i}{\sqrt{m_i}} (q_{ix}^l - iq_{iy}^l) \right|^2$, then the total transverse Einstein absorption coefficient is

$$B_T = (2) \frac{8\pi^3}{\hbar^2} \frac{\hbar}{4\omega_{l,\theta=\psi}} \left| \sum_i \frac{e_i}{\sqrt{m_i}} \frac{(q_{ix}^l + iq_{iy}^l)}{2} \right|^2. \tag{17}$$

The results of our calculation are shown in figure 1. We have plotted $|<\mu>|^2$ since the Einstein coefficient is simply a multiple of that value. The absorption peaks found by Powell, et.al.,[5] in irradiating Na - poly(dA) · poly(dT), are at 63, 83, 86, 100, 110 wavenumbers (cm^{-1}) at a temperature of 7 K as shown in figure 2. Our calculation in that region yields sizable peaks at 39, 45, 83, 89, 100, 109, 110 cm^{-1} for $\theta=\psi$ and 100 cm^{-1} for $\theta=0.0$. The polarization selections are different for the $\theta=0.0$ and $\theta=\psi$ modes. For absorption at $\theta=0.0$, the incident electric field must be parallel to the helix axis. For the incident field, perpendicular to the helix axis in the ordered film, the absorption is at $\theta=\psi$. The relative contributions to each depends on experimental details. We see no peak at 63 cm^{-1} and do not have a mode at 63 cm^{-1}. However, outside the range of possible observations in the infrared absorption experiment, we have two highly absorbing modes at 39, 45 cm^{-1}.[21] Using the

eigenvectors of the modes, we find the largest amplitude motion of the free phosphate oxygens occuring in the 39, 45 cm^{-1} modes (the motion being in the adenine backbone for 39 cm^{-1} and in the thymine backbone for 45 cm^{-1}). These modes are particularly likely to be affected by interhelical interactions as the phosphate groups are on the outside of the helix and highly charged. In packing two right-handed helices parallel to each other, regions of close contact between helix backbones necessarily occur as they must cross each other or distort from helical symmetry. It is likely that such modes are pushed up in frequency by interhelical interactions. We will return to this point when we discuss our calculation with interhelical interactions.

Counterions

A solution of DNA requires counterions for stabilization, but we have not included the presence of these ions explicitly in our earlier models. Simulations by Clementi and Corongiu[22] indicate that sodium counterions, strongly attracted to the free phosphate oxygens, follow helical patterns along the backbones. Such interactions with the phosphate groups could alter the frequency of phosphate vibrational modes.

The most difficult step in adding counterions to our model is determining their positions relative to our present set of coordinates. We placed sodium ions an average distance of 2.7 Å away from the free phosphate oxygens, one counterion for each phosphate group. This distance is in approximate agreement with calculations by Clementi and Corongiu.[22] Once the positions are found, the force constants can be calculated. It is likely that the main interaction of the ions and helix is via electrostatic forces. Addition of counterions requires an increase in the size of $[\mathbf{B}^t(\theta)\mathbf{F}\mathbf{B}(\theta)]_{nl}$, the non-bonded term in the

secular equation. The new elements for **B** and **F** are calculated as before in the non-bonded case, the ions interacting with the DNA atoms as well as other ions over four turns of the helix.

Solving this secular equation at $\theta=\psi$ yields eigenfrequencies of 34, 40, 47, 54 cm^{-1} in the range of interest, 34-65 cm^{-1}, as compared with 39, 45, 51, 54 cm^{-1} for the bare helix. The addition of counterions yields no mode near 60 cm^{-1}. Calculation of the absorption with these eigenvectors does show a decrease in the intensity of the peaks 34-50 cm^{-1},[21] while that of the mode at 54 cm^{-1} and the modes in the 80 cm^{-1} region showed sharp increases in absorption. The exception is the decrease in absorption of the mode at 74 cm^{-1}. In particular, the absorption of the mode at 89 cm^{-1} has more than tripled, while the mode at 83 cm^{-1} shows only a slight increase in absorption. Instead of one peak at 100 cm^{-1}, we find three -- 98, 99, 101 cm^{-1} -- and none at 110 cm^{-1}. The values of $|\langle\mu\rangle|^2$ for the modes in the range of 50-115 cm^{-1} are shown in figure 3.

Spine of Hydration

The water molecules of the solution which surround the atoms of DNA form hydrogen bonds with some of the nitrogen and oxygen atoms, the bond lifetime being about 10^{-11} seconds.[3] Thus, for frequencies greater than a few wavenumbers, this layer of water molecules is part of the DNA structure. Kopka, et.al.[23] describe the most distinct pattern of water molecules in B poly(dA) · poly(dT) as a "spine of hydration". In her data the spine is formed by water molecules which zig-zag from base pair to base pair along the helix axis in the minor groove. Between two base pairs, a water molecule forms a hydrogen-bond with a thymine O2 atom in one base pair and an

adenine N3 atom in the neighboring base pair. All along the helix, water molecules are found joining neighboring A-T base pairs. Then to complete the spine, these water molecules are connected to each other by forming hydrogen bonds with another water molecule located between those which bond to the bases (figure 7 of Kopka, et.al.[23]).

Aside from this distinct pattern, a total of about 20 water molecules per base pair are found. We limit ourselves to including only the "spine of hydration" in our model, the difficulty being the placing of the molecules in our unit cell configuration which is not exactly the same as the crystal configuration of Kopka et.al.[23] Then we calculate the modes for a system of DNA, ions, and this chain of water molecules interconnected by hydrogen bonds which approximates the spine. The hydrogen bond lengths for our calculation vary from 2.64 to 2.89 Å. We use the Lippincott-Schroeder model[24] to calculate the hydrogen bond stretch force constants which vary from 0.66 (for the 2.64 Å bond) to 0.08 $\frac{mdyne}{\text{Å}}$ (2.89 Å bond). We then approximate the angle bend force constants by taking the average of the stretch force constants of the bonds involved in the angle bend and then dividing by seven. The choice of $\frac{1}{7}$ of the magnitude of the stretch force constants is based on our comparison of the valence angle bend and stretch force constants. These approximated angle bend force constants vary in strength from 0.05 to 0.09 $\frac{mdyne\ \text{Å}}{rad^2}$. Because of the hydrogen bonding of the water molecules to certain DNA atoms, we increase the size of the bonded term in the secular equation, $[\mathbf{B}^t(\theta)\mathbf{F}\mathbf{B}(\theta)]_{ij}$. The hydrogen bond force constants are placed along the diagonal of F and the elements of B are calculated as before. Including the mass of the hydrogen atom of the water with its oxygen atom, we carry out the normal

mode calculation. Using these new eigenvectors, we then calculate the absorption. Although we now see a mode in the 60 cm^{-1} range (at 67 cm^{-1}), it shows relatively little absorption.[21] In the range 70-110 cm^{-1} we have significant peaks at 82, 86, 98, 110. In general, the absorption has decreased relative to the bare helix calculation, although the 86 cm^{-1} mode is as absorbing as the 89 cm^{-1} mode of the bare helix and the mode at 110 cm^{-1} shows an increased absorption.

Ions Plus Spine of Hydration

Each time an atom is added to the model, the size of the dynamical matrix, $\mathbf{B}^{\dagger}(\theta)\mathbf{F}\mathbf{B}(\theta)$ increases. Its rows and columns correspond to the numbering of the MWC coordinate components of the atoms. Adding ions increased $\mathbf{B}^{\dagger}(\theta)\mathbf{F}\mathbf{B}(\theta)$ through the non-bonded term, while adding water molecules increased $\mathbf{B}^{\dagger}(\theta)\mathbf{F}\mathbf{B}(\theta)$ through the bonded term. Thus, when we find the secular equation for this system by adding the two terms, we must make sure the ion and water matrix elements do not overlap. The addition of two ions and two water molecules per unit cell increases the size of the final matrix for the unit cell from 123x123 to 135x135. The eigenvectors from this calculation yield a further reduction in absorption of the 66 cm^{-1} mode (from $0.25\text{x}10^{-20}$ to $0.03\text{x}10^{-20}$ $(e-cm)^2$, where e is the electronic charge).[21] As would be expected, in general, the absorption has decreased relative to the calculation in which ions alone are added and increased relative to the calculation in which water molecules alone are added. Specifically, in the 70-110 cm^{-1} region, the modes with significant peaks are at 81, 86, 90, 97, 99, 101, 103 cm^{-1} as shown in figure 4.

Although the addition of ions does seem to affect the modes with large amplitude motion of the free phosphate oxygens, and the addition of water molecules does give a mode near 63 cm^{-1}, such results are still not in good agreement with the experimental observation of a highly absorbing peak at 63 cm^{-1}. More likely, some other mechanism will move the 39, 45 cm^{-1} modes to higher frequency -- namely, interhelical coupling.

Interhelical Coupling

Another mechanism for stiffening of the 39, 45 cm^{-1} modes is an electrostatic interaction between the phosphate groups of different helices with the sodium counterions included. One can make a crude attempt to model such a coupling by using transverse periodic boundary conditions. We essentially generate an infinite array of base pairs (including a sodium ion at each phosphate group) along $\hat{y}$ in one base pair's (or unit cell's) frame of reference, where $\hat{y}$ is approximately parallel to the interbase hydrogen bonds. Then we take this array and repeat it along the original base pair's helix axis by the translations and rotations that give DNA its helical symmetry. Of course, we have not succeeded in generating separate helices, but this model should still be valid to look at the effect of the interaction of phosphate groups of nucleotides of different helices on the motion of the free phosphate oxygens. Lindsay[12] provides the distance between helix axes from fiber diffraction experiments. We use 28 A as this distance; that is, in generating the transverse array of base pairs, the distance between the helix axis of each base pair is 28 A.

We use the same electrostatic formalism as for the calculation of the addition of counterions to the model. This time the interaction is between the ± 1

transverse repeat unit and the initial repeat unit (cell 0), where ±1 refers to a translation of $\pm 28\text{Å}\hat{y}$. Another modification is due to the amount of phosphate clashing between helices. Our model includes a clash for each phosphate group, but such clashes should only occur approximately every five vertical unit cells for neighboring helices. For this reason, we decrease the force constants by $\frac{1}{5}$ to improve the frequencies, realizing that details of our calculation, such as amplitudes of specific atomic motion will be less meaningful.

In the range of interest, interhelical coupling yields modes at 33, 40, 45, 50, 52, 60, 61 cm^{-1}.[21] These modes show less motion for the free phosphate oxygen atoms. The modes at 40, 45 cm^{-1} are now less absorbing than the 39, 45 cm^{-1} modes of the bare helix. Also, we now have modes with higher absorption in the 50 - 65 cm^{-1} range (figure 5), whereas before, with the bare helix, we had no greatly absorbing modes in that region. With the addition of ions, only one significantly absorbing mode appeared in that range. In fact, the absorption of the 52 cm^{-1} mode is near the magnitude of that of the 40 and 45 cm^{-1} modes. In the 70-100 cm^{-1} range, the effect on the peaks relative to the bare helix is similar to that of adding counterions alone, except that the modes are shifted slightly higher: 84, 89, 98, 100, 103 cm^{-1}.

Conclusions

We do find that our single helix calculations fit fairly well the observed modes believed to be intrahelical. This result is likely as the modes calculated in this frequency regime are principally stretch modes of the interbase hydrogen bonds. The fact that even the addition of counterions and water molecules shifts these modes by only a few wavenumbers reinforces their

assignment as hydrogen bond stretches. Also, these modes are not strongly connected to interhelical interactions. The explicit addition of a few counterions and water molecules affects the interhelical modes very little as well.

When interhelical coupling is added modes are shifted in frequency. This effect is expected to be particularly important in those cases where the helices are relatively well ordered. Most importantly, these well ordered cases are the ones that lead to the best resolved spectra. The evidence is that one needs to take into account the interhelical interactions to explain the best spectral data. We see that shifts in frequency of the order needed to obtain better agreement with experiment can be obtained with crude approximations of the interhelical interactions.

This crude calculation of interhelical effects has several flaws which make the calculation suspect and in particular the calculation of the absorption is inaccurate. Adding the transverse array of nucleotide pairs to approximate interhelical coupling actually creates a new molecule altogether. Thus, the symmetry is not the symmetry of the original system. The eigenvectors in particular will be incorrect, although the frequencies may be close to those of a system with interhelical effects. The eigenvectors, however, are what are important in calculating absorption strength. More sophisticated calculations which include interhelical effects are in progress.

Acknowledgements

We wish to thank Professor K.S. Girirajan for the use of his variable dielectric models. We also wish to thank Professor John Powell for permission to use figure 2 Powell, et.al. on the observed far infrared absorption. This work was supported by NIH grant GM24443 and ONR grant N00014-86-K-0252.

References

1 E.W. Prohofsky, K.C. Lu, L.L. Van Zandt, B.F. Putnam, Physics Letters 70A, 492-494 (1979)

2 K.V. Devi Prasad, and E.W. Prohofsky, Biopolymers 23, 1795-1798, (1984)

3 N.J. Tao, S.M. Lindsay, A. Rupprecht, Biopolymers 26, 171 (1987)

4 Y. Tominaga, M. Shida, K. Kubota, H. Urabe, Y. Nishimura, M. Tsuboi, 83, 5972-5975 (1985)

5 J.W. Powell, G.S. Edwards, L. Genzel, F. Kremer, A. Wittlin, W. Kubasek, W. Peticolas, Physical Review A 35, 3929-3939, (1987)

6 Y. Kim, K.V. Devi Prasad, E.W. Prohofsky, Physical Review B 32, 5185-5189 (1985)

7 H. Grimm, H. Stiller, C.F. Majkrzak, A. Rupprecht, U. Dahlborg, Phys. Rev. Lett. 59, 1780 (1987)

8 V.V. Prabhu, W.K. Schroll, L.L. Van Zandt, E.W. Prohofsky, submitted for publication

9 V.V. Prabhu and E.W. Prohofsky, private communication

10 S.A. Lee, S.M. Lindsay, J.W. Powell, T. Weidlich, N.J. Tao, G.D. Lewen, and A. Rupprecht, Biopolymers 26, 1637-1665 (1987)

11 K.C. Lu, E.W. Prohofsky, L.L. Van Zandt, Biopolymers 16, 2491-2506 (1977)

12 S.M. Lindsay, to be published in Computer Analysis for Life Science, Ohm, Tokyo, (1985)

13 J.M. Eyster and E.W. Prohofsky, Biopolymers 13, 2505-2526, (1974)

14 J.M. Eyster and E.W. Prohofsky, Biopolymers 16, 965-982, (1977)

15 E.B. Wilson, J.C. Decius, and P.C. Cross, Molecular Vibrations, Ch. 4, Dover Publications, New York, (1980)

16 K.J. Miller, Biopolymers 18, 959-980, (1979)

17 D.A. Pearlman, S.H. Kim, Biopolymers 24, 327-357 (1985)

18 A.J. Hopfinger, Conformational Properties of Macromolecules, Academic Press, New York, Chap. 2, Sec. VI, (1973)

19 K.S. Girirajan and E.W. Prohofsky to be published

20 M. Kohli, W.N. Mei, E.W. Prohofsky, and L.L. Van Zandt, Biopolymers 23, 853-864, (1981)

21 L. Young, Ph.D. Thesis, Purdue University, in progress.

22 E. Clementi, G. Corongiu, IBM DPPG Research Report POK-1, (1981)

23 M.L. Kopka, A.V. Fratini, H.R. Drew, R.E. Dickerson, J. Mol. Biol. 163, 129-146, (1983)

24 R. Schroeder, and E.R. Lipppincott, J. Phys. Chem., 61, 921-928, (1957)

Figure Captions

Figure 1. The dotted lines represent the square of the dipole moment matrix element for each longitudinal (θ= 0.0) mode of poly(dA) · poly(dT) in the 50 - 115 cm^{-1} range. The solid lines are for the square of the dipole moment matrix element for each transverse (θ=ψ) mode of poly(dA) · poly(dT) in the 50 - 115 cm^{-1} range. The square dipole moment unit is $(e \cdot cm)^2$.

Figure 2. The locations of the peaks in the measured absorption spectrum of Powell, et.al.[5]

Figure 3. The absorption is given as in figure 1 for the transverse modes, but with the addition of counterions.

Figure 4. The absorption is given as in figure 1 for transverse modes, but with the addition of counterions and the addition of water molecules binding to atoms in the bases and to each other.

Figure 5. The absorption is shown as in figure 1 for transverse modes, but with interhelical coupling.

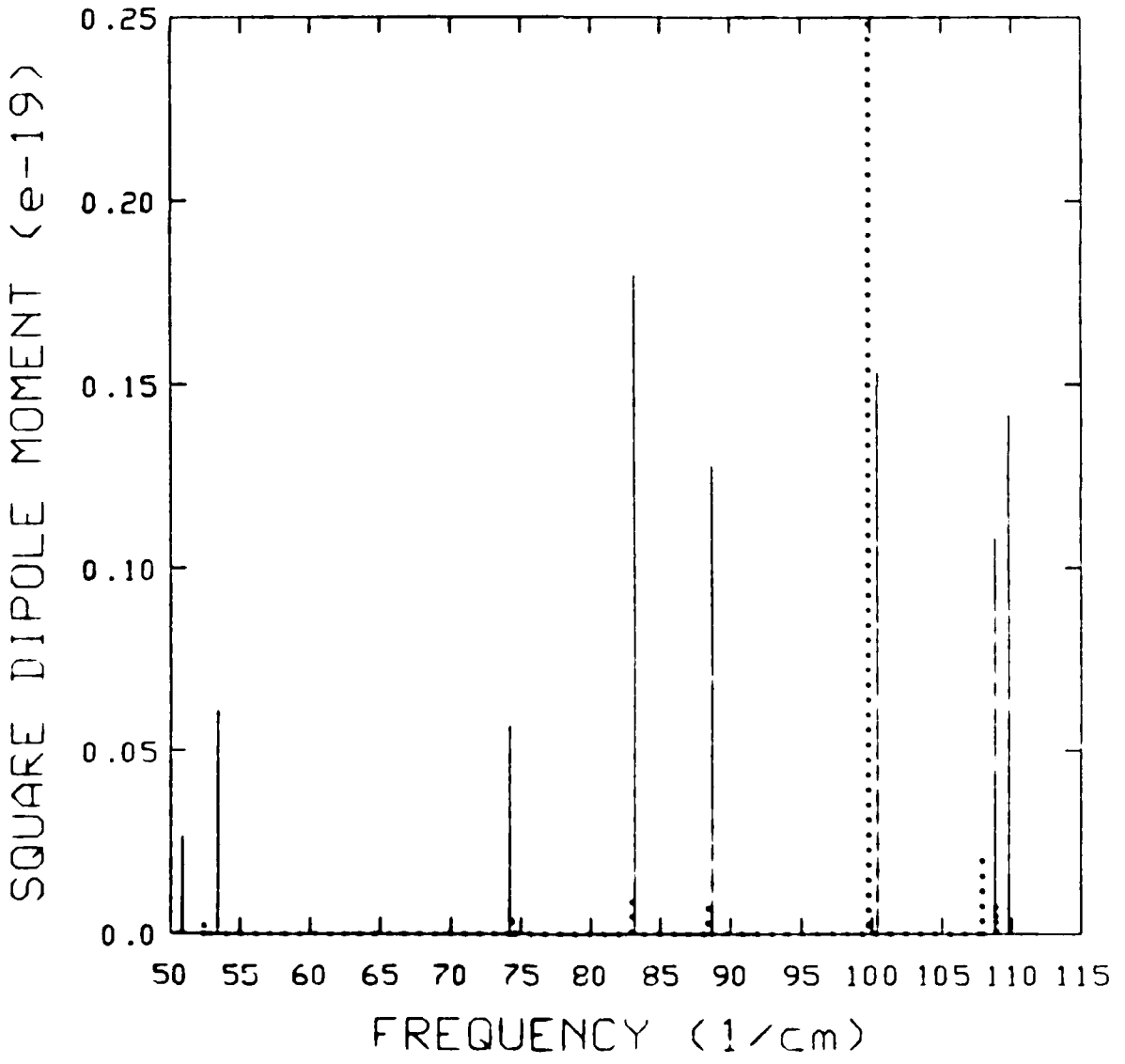
SQUARE DIPOLE MOMENT (e-19)
0.25
0.20
0.15
0.10
0.05
0.0
50 55 60 65 70 75 80 85 90 95 100 105 110 115
FREQUENCY (1/cm)

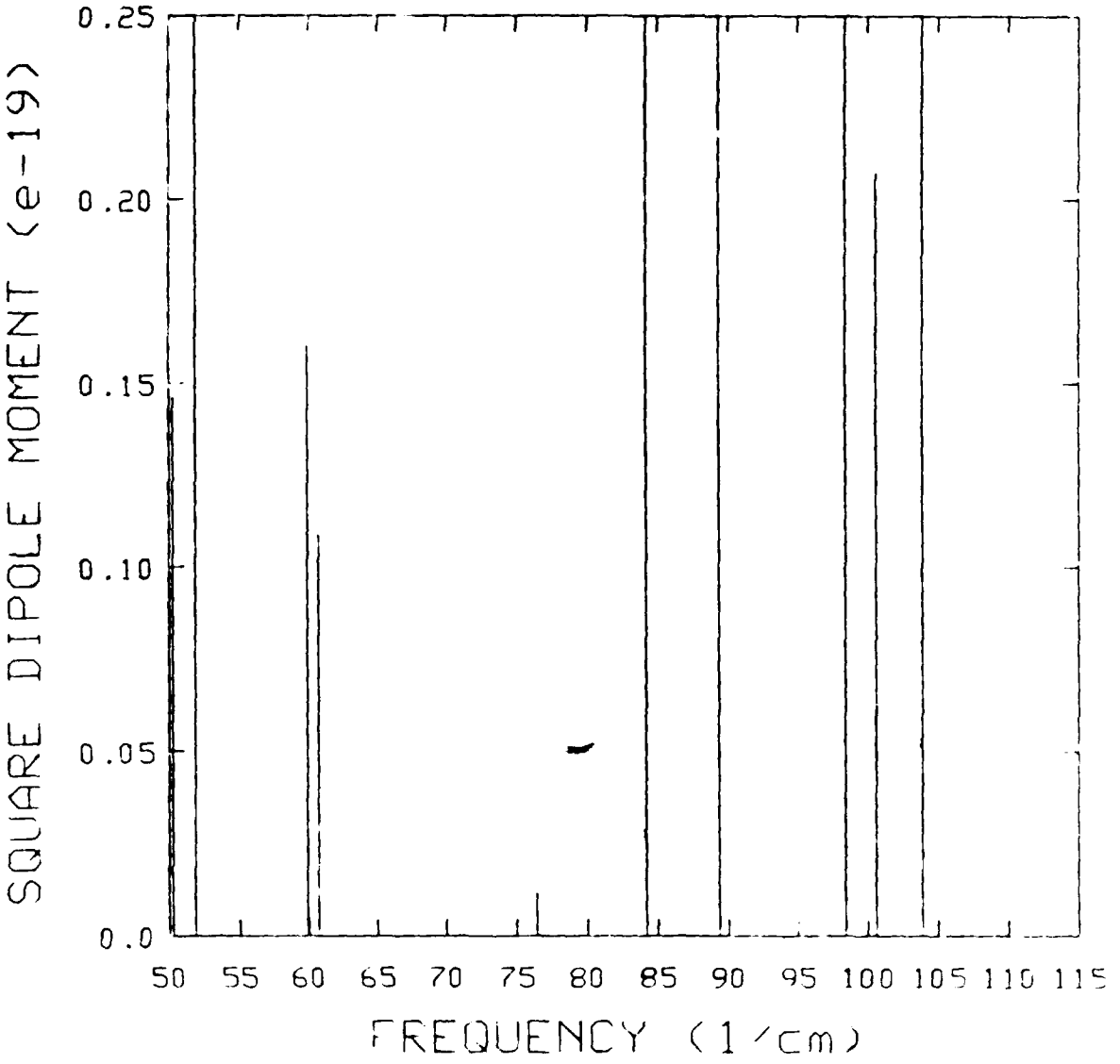
SQUARE DIPOLE MOMENT (e-19)
0.25
0.20
0.15
0.10
0.05
0.0
50 55 60 65 70 75 80 85 90 95 100 105 110 115
FREQUENCY (1/cm)

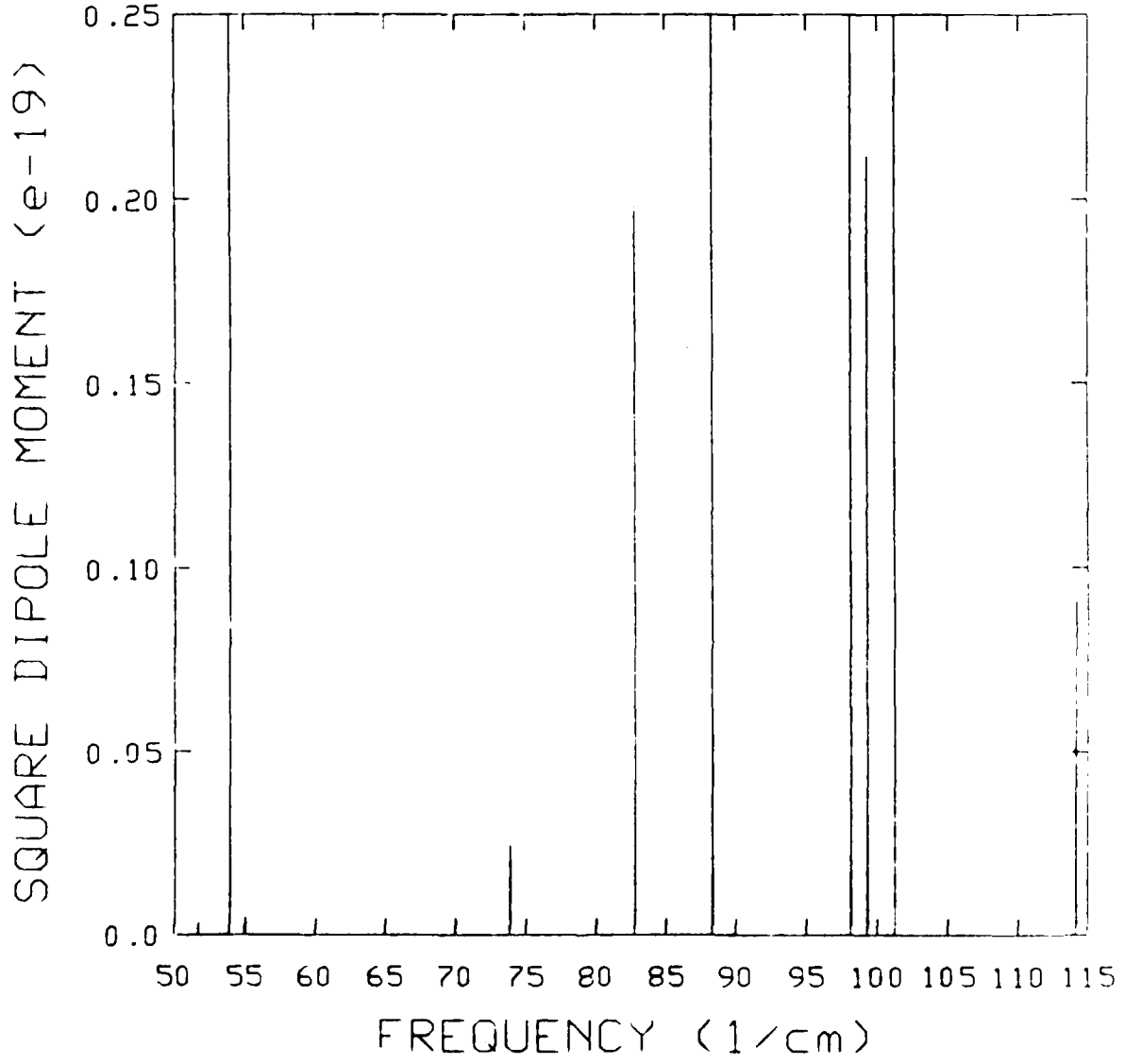
SQUARE DIPOLE MOMENT (e-19)
0.25
0.20
0.15
0.10
0.05
0.0
50 55 60 65 70 75 80 85 90 95 100 105 110 115
FREQUENCY (1/cm)

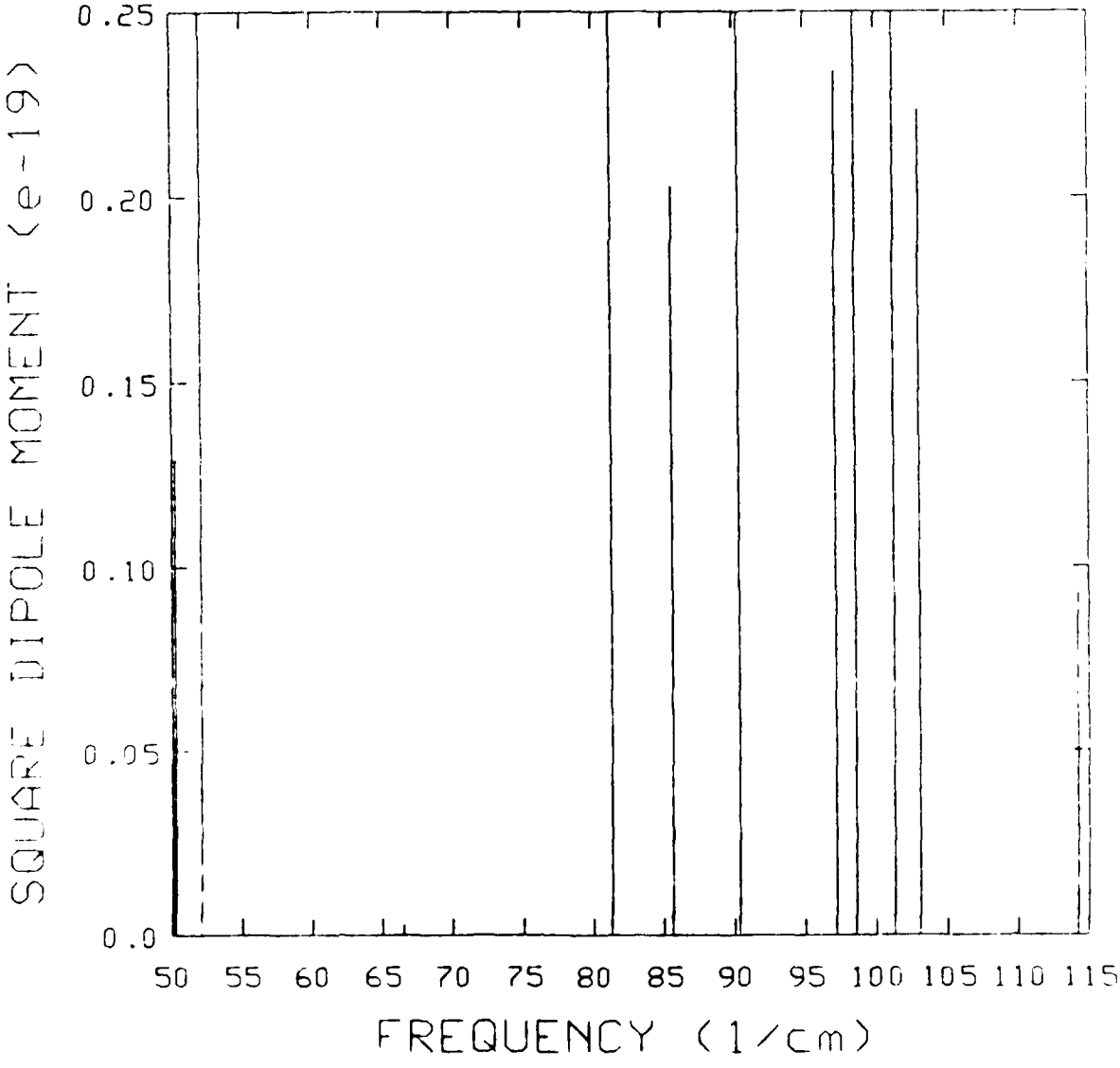
SQUARE DIPOLE MOMENT (e-19)
0.25
0.20
0.15
0.10
0.05
0.0
50 55 60 65 70 75 80 85 90 95 100 105 110 115
FREQUENCY (1/cm)

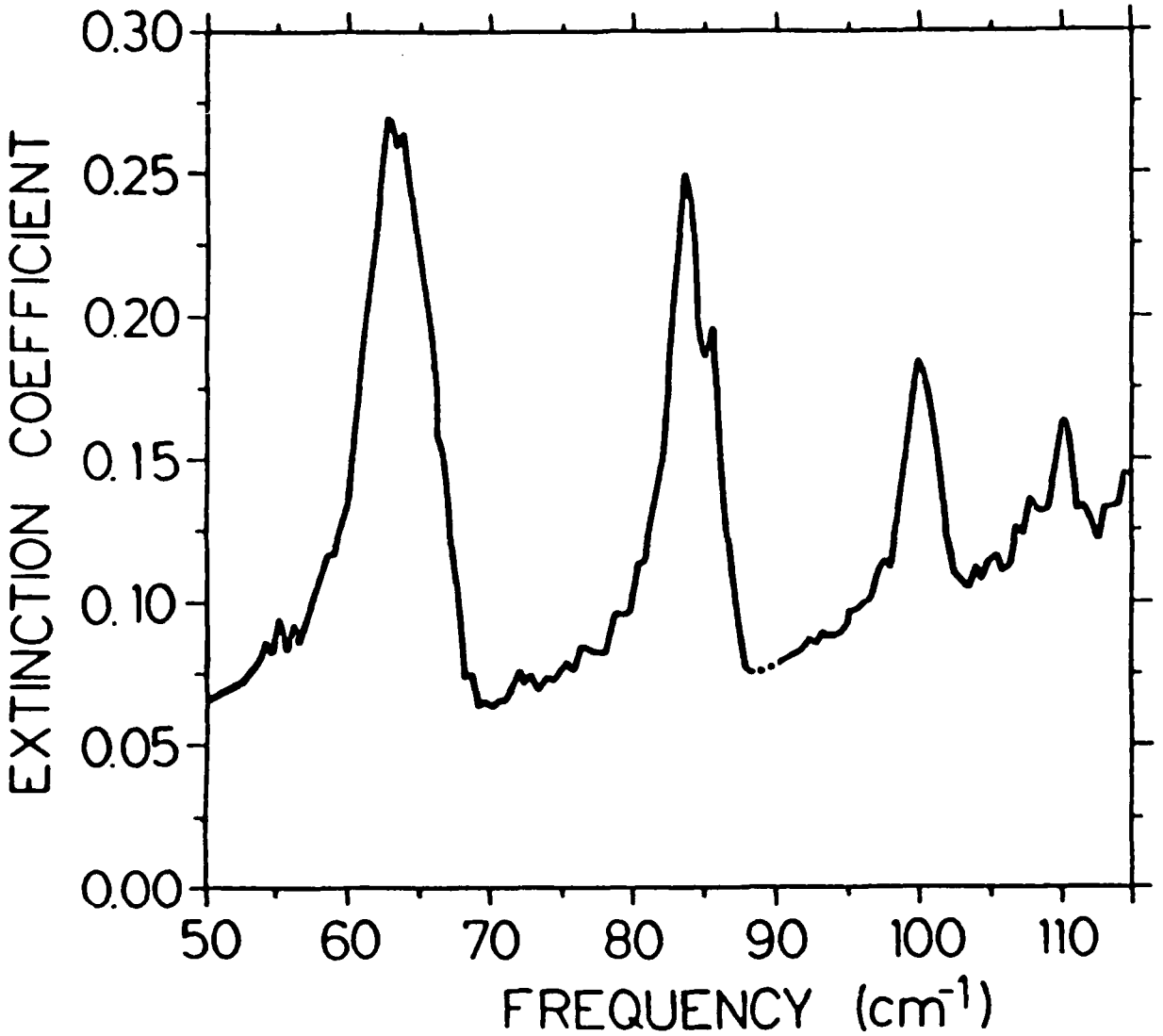
0.30
0.25
0.20
0.15
0.10
0.05
0.00
EXTINCTION COEFFICIENT
50
60
70
80
90
100
110
FREQUENCY (cm-1)

END

DATE

FILMED

DTIC

JULY 88